

Temperature spatial variability analysis in the aim of enhancing the use or implementation of wind machines park

Clara Le Cap (✉ clara.le-cap@inrae.fr)

Weather Measures

Johan Carlier

National Research Institute for Agriculture, Food and Environment

Hervé QuénoI

French National Centre for Scientific Research

Dominique Heitz

National Research Institute for Agriculture, Food and Environment

Emmanuel Buisson

Weather Measures

Research Article

Keywords: temperature spatial variability, hierarchical clustering, frost, wind machine, vineyard of Quincy

Posted Date: August 10th, 2022

DOI: <https://doi.org/10.21203/rs.3.rs-1932104/v1>

License:   This work is licensed under a Creative Commons Attribution 4.0 International License.

[Read Full License](#)

Version of Record: A version of this preprint was published at Theoretical and Applied Climatology on September 21st, 2023. See the published version at <https://doi.org/10.1007/s00704-023-04642-7>.

Abstract

Spring frosts after budburst are responsible for crop losses and threaten local economies. As global warming tends to advance the phenological stages of plants, these become more and more subject to facing a long period of freezing temperatures. For a given meteorologic situation, the topography of the studied site and the nature of the soil of the plots constituting it, a temperature spatial variability expands within the same territory. Considering a radiative frost, the temperature can thus differ by several degrees, creating areas of cold and warm air that it is necessary to know to fight wisely against the frost.

Nowadays, many solutions exist to fight against frost, including the wind machines that dot the Quincy vineyard in France. Weather variables, topographic parameters, and daily minimum temperatures from a network of connected sensors scattered throughout the vineyard are retrieved for the last three spring seasons of 2020, 2021, and 2022. Then, thanks to a hierarchical clustering algorithm, it is possible to link the spatial variability of temperatures to the synoptic situation and the topography of the domain. The outcome is the assessment of the frost risk areas to propose a judicious implantation of wind machines in the vineyard of Quincy.

1 Introduction

Each year, spring frost causes a huge economic loss in agriculture due to the early growing of plants. Climate change is characterized by the increase of the mean temperature on the planet's surface. Across the world, the impact is felt at all scales, such as the wine sector. The effects of climate change on the spatial distribution of frost and its consequences on crops, and potential expansion are therefore highly studied. Gobbett et al. (2020) presents a high-resolution spatial analysis of frost distribution based on remotely sensed land surface temperature (MODIS) data and Multivariate Adaptive Regression Splines (MARS) method, while Webb et al. (2018) proposes a mapping of frost risk by spatially linking minimum temperature records and bud break dates. Mosedale et al. (2015) demonstrates how stochastic weather generators can be used to predict future suitable growing areas using the example of viticulture in southwest England. But if the geographical consequences are easily understandable, climate change also has a significant effect on the phenology of plants and it is the combination of the two that concerns the wine community. Vine plants phenology can be divided into 4 events of dormant phase, budburst, floraison and veraison (Hellman, 2000; Jones and Davis, 2000). The budburst happens after the plant has stored a sufficient amount of heat to grow. Several studies showed that the climate change is causing certain phenological stages of the plants to advance (Augspurger, 2013; Unterberger et al., 2018; Van Oldenborgh and Li, 2022) and winegrowers began to observe budburst at unexpected early season (Leolini et al., 2018; Sgubin et al., 2018).

Besides, global warming can be highlighted in various ways but one singularity is the continuous increase of extreme temperatures occurrences and their fellow intensities. It results in strong variability of spring frost event frequency, particularly in Europe where different climates are represented (Leolini et al., 2018; Zohner et al., 2020). Indeed, some regions are predicted to face more spring frost events in the near future while others may observe the decrease of their occurrences (Leolini et al., 2018; Ma et al., 2019;

Meier et al., 2018; Unterberger et al., 2018; Zohner et al., 2020). But if freezing temperatures still occurs in the late night, so does unusual positive ones during the day, thus disrupting the phenology of the plants. While the vine plants are cold hardy during dormancy, as soon as budburst occurs, their cold resisting ability decreases as their growing cycle go forward (Quénol et al., 2004). It makes the early buds very vulnerable when they have to go through freezing temperatures. Then, for the sustainability of orchards, it becomes vital to assess the temperature spatial variability and therefore the current (Cittadini et al., 2006; Detzer et al., 2020) and future frost risk (Gavrilescu et al., 2019) to adapt cultivation practices, frost control systems, and even insurance policy (Zohner et al., 2020).

A strong spatial temperatures variability can be assumed in a limited territory depending on several parameters. Frosts can be distinguished as advective frosts and radiative frosts:

- Advective frost is caused by an arrival of a cold mass of air (wind > 3 m/s) mixing the atmosphere, thus inducing the cold establishment on a whole crop. Therefore, the temperature spatial variability is weak, and damages are generalized in the vineyard;
- Radiative frosts are characterized by clear skies and shallow winds (wind < 2 m/s), which results in energy loss near the ground after sunset. Indeed, soil heatwaves gradually fade away to the sky, thus creating a thermal stratification in the low part of the atmosphere (from a few meters to several hundreds of meters above the ground). This thermal inversion is responsible of frost which could occur in the late night (Quénol et al., 2004).

Depending on the type of frost occurring, but also the synoptic situation and local parameters such as topography, the minimum temperature can differ by several degrees within the same vineyard. As a matter of fact, katabatic drainage, defined as a flow of cold air along the slopes tends to create lakes of cold air in the valley bottoms where cold air can accumulate, while the highlands are spared (Kalma et al., 1992). It leads to observations of strong minimum temperature spatial variability due to the topography (Quénol et al., 2004; Small, 1949).

Hence, for many years, men have been developing new solutions to counter this seasonal phenomenon by adopting strategies of cultural practices but also by designing technologies that help them to overcome this biological and economic disaster (Snyder and de Melo-Abreu, 2005). Although no adequate solution exists to fight the advective frost, numerous solutions appeared over time to counter radiative spring frost such as candles, sprinkling water or wind machines. These solutions have proven their efficiency and are chosen according to different constraints (Lakatos et al., 2016). For instance, sprinkling requires a highly available water reserve during the whole freezing episode while candles must be renewed regularly during the night. Wind machines represent a significant financial investment and require the presence of thermal stratification to be effective. The utility of wind machines is then conditioned by a climatological assessment where minimum temperature and inversion strength are cornerstones (Doesken and McKee, 1988). Therefore, their implementation must be carefully considered and it is necessary to study the spatial variability of frost to obtain a maximum performance. Down through the years, as the budburst occurs at an increasingly early stage, the fight against frost must be

maintained much longer to cover longer nights than usually known by the winegrowers. Hence, some historic solutions become more challenging to use, because of their limited use duration. Therefore, using a wind machine appears as a great solution to protect vineyards and orchards, as it can work as long as required by the weather conditions (Kalma et al., 1992).

Various types of wind machine exist on the market, such as portable wind machine or upward blowing wind machine, but several studies showed that stationary wind machine as can be founded in the Quincy vineyard is the more efficient to fight spring frost (Battany, 2012; Beyá-Marshall et al., 2019) whether in terms of range or thermal gain magnitude.

A wind machine is commonly composed of a 10-m mast and a 2-bladed-hub blowing fan at its peak. The wind machine rotates on itself in 4–5 min. The operation of a wind machine is conditioned by the state of the atmosphere as it requires a minimum thermal inversion of 1.5°C – 2°C between 1.5 m and 15 m high (Kalma et al., 1992). The blowing fan sweeps the crop by blending warm air quickly above with the cold air near the ground (Bates and Lombard, 1978; Brooks et al., n.d.).

Wind machines offer protection to orchards but with slight differences depending on the thermal inversion strength (Bates and Lombard, 1978; Evans, 2000; Ribeiro et al., 2006). Moreover, every study carried on with field measurements showed that the wind machine produces a strong spatial variability of temperature, with a decreasing effect with the distance to the fan but also in height (Beyá-Marshall et al., 2019; Heusinkveld et al., 2020; Ribeiro et al., 2006). Consequently, damages observed on flowers were minor near the fan but increased with the distance (Ribeiro et al., 2006).

Furthermore, the natural wind drift seems to be prevailing in the spatial variability of temperatures gain produced by the wind machine. A light wind tends to extend the range of the wind machine's jet downwind and shorten it both upwind and perpendicularly (Beyá-Marshall et al., 2019; Heusinkveld et al., 2020; Ribeiro et al., 2006). Obviously, a value above 1.8 m/s prevents stratification and thus the ignition of the wind machine. On the other hand, To enhance the protection and its coverage, multiple wind machines can also work together in a synergy effect (Beyá-Marshall et al., 2019; Snyder and Melo-Abreu, 2005).

Despite a growing interest in wind machines effect to protect crops, no study covered the possible improvement of their use or locations regarding the natural temperature spatial variability. The present study aims to analyze the spatial variability of temperature using hierarchical clustering (Murtagh and Contreras, 2012) and a network of connected sensors to propose a well-considered implementation of wind machines. This study is carried out in the Quincy vineyard, where nearly 60 wind machines are disseminated, offering protection against spring frost for 85% of the crop. We focus on the statistical analysis of the minimum temperature spatial variability following several atmospheric situations in the Quincy vineyard during spring frost occurrences in 2020, 2021, and 2022. In section 1 we present an overview of the site and methods. The results are shown and analyzed in section 2. Finally, we draw some conclusions and perspectives in section 3.

2 Site And Methods

In the vineyard of Quincy, wind machines (WM) have been in use since the early 2000s. From a single one, there are today nearly sixty of them throughout the vineyard. They were implanted based on accessibility, social connections through membership in the local agricultural cooperative, and winegrowers' field experience. But not in the context of global warming prone to change the well-known risk areas. Today, some towers are equipped with a sensor allowing them to be switched on automatically when the temperature falls below a critical threshold, but others still require human intervention in their use. To fight spring frost, in addition to their knowledge, the winegrowers of Quincy use weather forecasts and a network of temperature sensors spread throughout the vineyard as a decision-making tool.

2.1 Site of study and data

Figure 1 shows on the left the location of the Quincy vineyard in the Centre Val de Loire region in France where the study was conducted. On the right, the wind machine locations among temperature sensor locations are displayed on the vineyard map. The Quincy vineyard covers a delimited zone of 700 Ha. It benefits from a moderate climate and a sandy and gravelly soil settled in old alluvial earthworks perched on riparian limestone hillsides. The wine of Quincy is a white wine with registered designations of origin based upon the particular Sauvignon vine variety. Vine stocks are planted with a spacing of 1 m to 1.15 m between plants and 1.5 m between rows.

Synoptic Data - Weather conditions

Meteorologic regional variables were considered from the national weather station of Bourges, located approximately 22 km from the vineyard. Nebulosity data came from the AROME forecast model with a spatial grid of 2.5 km. Each night, several weather variables were retrieved, such as the wind speed and direction, pressure, humidity, and nebulosity. Besides, an adding variable was defined and could take three values depending on the evolution of the nebulosity: -1, meaning the sky was revealed at night, 0, no change, and 1, the sky became overcast during the night.

Micro meteorological measurements

A wireless sensors network was settled in December 2019 to monitor the temperature across the vineyard and alert when the temperature drops too far. Thirty-seven of these Weenat[↔] anti-frost sensors are spread in the whole vineyard and measure the temperature continuously. The locations of these sensors are shown above in Fig. 1. By retrieving the hourly temperatures of the remote sensors, the daily minimum temperature can be extracted, which is defined as the minimum temperature measurement between 6 pm the day before and 6 pm the same day.

Topographic data

Figure 2 presents histograms of topographic data at Weenat[↔] sensor locations in the Quincy vineyard. Topographic data are described by Digital Elevation Model (DEM) and are 5-m accurate. The vineyard of

Quincy is located in a flat area as its slope varies between 0° and 6°, with a majority of values between 0° and 3° (see Fig. 2b). The mean altitude is 122 m, and the main exposure varies between North and East. Besides altitude and slope, it also allows for analyzing the plots' exposure (see Fig. 2c and 2d). However, exposure values can be tricky to analyze for a statistical algorithm, especially when a wind from extreme compass points is recorded. As explained in Le Roux, 2017, a wind with an angle of 359° or 1° both mean that wind is coming from the north direction, but it will be interpreted as two very different wind flows by the algorithm. To prevent this issue, one should decompose the direction as two components ranging between - 1 and + 1, called U and V, with U corresponding to the north/south orientation and V to the east/west orientation. To do so, $U = \cos(\text{angle in radian})$ and $V = \sin(\text{angle in radian})$, with $U = 1$ for northern orientation and $- 1$ for southern orientation, $V = 1$ for eastern orientation, and $- 1$ for western orientation.

2.2 Methods

Hierarchical Clustering (HC) is a statistical method used to group individuals according to similar variables that define them. Then, a dendrogram is obtained, which is divided into several clusters of individuals, each distinct from each other. Thus, each individual from the same cluster is assumed to be similar. This method allows to group nights of frost following weather variables, plots following the micro-scale temperature, and topographic parameters. So, the statistical analysis was based on different data sources:

- weather data;
- micro-scale temperature data;
- and topographic data.

Figure 3 indicates the four different steps the study goes through to analyze the temperature spatial variability in the Quincy vineyard during frost events. Each hierarchical clustering is performed using the “agnes” function (for “Agglomerative Nesting”) from the “cluster” library provided with the data-treatment software R.

First step corresponds to the analyze of the weather data, for each night of frost recorded in the Quincy vineyard during the three previous spring seasons. The application of the hierarchical clustering on these data allowed to identify different clusters of frost nights which could be then defined as either advective or radiative frost cluster or even a blend of the previous two types, depending on the characteristics of each cluster.

Step two focus on the topographic description of the vineyard. To that purpose, two topographic HC is performed, each one having a different set of parameters:

- The first one took into account all the topographic parameters provided by the DEM at sensor locations: altitude, slope, and exposure broken down into 2 components U and V.
- The second one only took into account the slope and the altitude

Step three considers the micro-scale temperatures provided by the Weenat temperature sensors. Once the frost nights clusters were defined in step one, the same pattern was applied on plots following the minimum temperature recordings through the wireless sensors network for nights from a same cluster. For instance, if the HC on frost nights resulted in 3 clusters: one for advective frost nights, one for radiative frost nights and the third for a blend of advective and radiative situations, then one would apply HC on plots following the minimal temperatures recorded during each type of frost. This second step allowed to determine hot and cold areas during a specific kind of frost and establish a relationship between micro-scale temperature distribution and observed weather.

Finally, in step four, we link the spatial variability of temperatures with topographic effects, by comparing the HC results from minimum temperature records in the vineyard (step 3) with the previous two topographic HC results (step 2). Having one topographic result taking exposure into account imply to observe the impact of wind and solar radiation on temperature by finding link between topographic and temperature HC, which is more likely to happen during advective or blurred frost situation. On the opposite, the same comparison with altitude and slope only is more relevant for radiation frost occurrence as temperature distribution is strongly dependent of terrain shape.

3 Results And Discussion

In this section, we detail the results of the different steps of the methodology presented above before linking each one. Then, we will compare the areas benefiting or not from the use of wind machines in order to reaffirm their interest. Finally, we compare the results of the different classifications with the current implementation of wind machines in Quincy and bring our observations and suggestions.

3.1 Synoptic HC results: Evidence of 3 types of frost

Figure 3, Step 1 refers to the study of the temperature variability across the vineyard for different frost type occurrences. Hierarchical clustering was carried out on synoptic data: wind speed and direction, humidity, pressure, and nebulosity for the nights when frost was recorded. Several clusters of similar nights were obtained and allowed to identify the types of frost events that occurred on those nights.

Thirty-four nights of frost were recorded in the Quincy vineyard in the last three springs: eleven in 2020, twenty-one in 2021, and only two in 2022.

The synoptic hierarchical clustering resulted in a three-cluster classification of frost nights with the following characteristics presented in Table 1 below. The nebulosity reduced thermal loss as cluster 2, which stands out from the other clusters with its high sky coverage, holds the hottest mean minimum temperature. As advective frost is characterized by the arrival of a cold mass of air carried along by strong winds, one could presume that the temperature should be pretty homogenous on a terrain, which was not observed in this study. Indeed, Cluster 1 represents nights where a blend of advective and

radiative situations occurred. However, this cluster presents the highest standard deviation value of the minimum temperature in the Quincy vineyard.

In contrast, its mean minimum temperature was close to the one of Cluster 3. Cluster 3 was characterized by light winds and moderate sky coverage, thinking that radiative frost occurred these nights. While it has been stated that the nebulosity affects the drop of the minimal temperature, it did not seem to affect the scattering of the temperature as this value is very close for clusters 2 and 3.

Table 1
HC results of frost nights recorded in 2020, 2021, and 2022 in the Quincy vineyard

	Cluster 1	Cluster 2	Cluster 3
Number of frost nights in the Quincy vineyard	11	13	10
Characteristics of the cluster	High wind speed from NE Low humidity Low sky coverage with no evolution during the night High-pressure situations	Reasonable wind speed from S / SO Humidity upper than average Blend of nights where the sky is clear or is strongly overcast with no evolution or an uncovering High- and Low-pressure situations	Light wind from SE Humidity upper than average Quite strong high-pressure situations The sky was overcast during the night but with a moderate coverage
Deduction of the type of frost	Mix of advective and radiative situation	Radiative with nebulosity	Radiative with a light sky covering
Mean minimal temperature in the vineyard	-1,75°C	-0,99°C	-1,82°C
Standard deviation of the minimum temperature in the vineyard	0,98°C	0,88°C	0.86°C

3.2 Topographic data

Figure 3, Step 2 refers to the clustering of plots according to topographic parameters. Topographic information was collected at temperature sensor locations within the plots constituting the vineyard from the 5-m accurate DEM. Bottom areas and high plateaus were identified as well as sloping and oriented fields. Later in this paper, topographic results are compared with micro-scale temperature HC results to

identify a similar pattern between temperature distribution and topographic shape for various types of frost defined in the first step of the analysis.

Table 2 presents the characteristics of topographic clusters produced by the HC algorithm for the two sets of parameters. The most relevant parameters are highlighted for each cluster following the p-value. Cluster 1 from the first hierarchical clustering was characterized by a high slope and low altitude, whereas Cluster 2 from the second hierarchical clustering was characterized by a low slope and high altitude. One should be vigilant about the order of magnitude of the standard deviation in category which is often close to the overall one. When comparing a temperature cluster with these two topographic clusters, it could happen that a majority of the plots could either be constituted of one or another and seemed conflicting. By comparing the value of each plot with the overall mean, a larger proportion of the percentage of plots was always found to be above or below the overall average. Results are then confirmed despite these two conflicting clusters.

Table 2

Characteristics of topographic clusters produced by the HC algorithm for the two sets of parameters

First Hierarchical Clustering					
Cluster 1					
	Mean in category	Overall mean	Standard deviation in category	Overall standard deviation	P value
Slope	2.83	1.82	1.35	1.33	0.00016
U	0.54	0.39	0.62	0.66	0.25
V	0.44	0.38	0.37	0.53	0.57
Altitude	118.30	122.4	5.68	6.69	0.0024
Cluster 2					
	Mean in category	Overall mean	Standard deviation in category	Overall standard deviation	P value
Slope	1.22	1.82	0.58	1.33	0.099
U	-0.36	0.39	0.37	0.66	3.019e-05
V	0.82	0.38	0.26	0.53	2.38e-03
Altitude	123.66	122.4	6.98	6.69	0.49
Cluster 3					
	Mean in category	Overall mean	Standard deviation in category	Overall standard deviation	P value
Slope	1.06	1.82	0.86	1.33	0.017
U	0.82	0.39	0.23	0.66	0.0061
V	-0.064	0.38	0.52	0.53	0.00052
Altitude	126.48	122.4	4.26	6.69	0.011
Second Hierarchical Clustering					
Cluster 1					
	Mean in category	Overall mean	Standard deviation in category	Overall standard deviation	P value
Slope	1.70	1.82	0.89	1.33	0.77
Altitude	112.58	122.4	2.58	6.69	3.78e-06

First Hierarchical Clustering					
Cluster 2					
	Mean in category	Overall mean	Standard deviation in category	Overall standard deviation	P value
Slope	1.24	1.82	0.73	1.33	7.35e-04
Altitude	125.55	122.4	4.90	6.69	2.88e-04
Cluster 3					
	Mean in category	Overall mean	Standard deviation in category	Overall standard deviation	P value
Slope	4.22	1.82	0.85	1.33	1.88e-06
Altitude	123.40	122.4	2.76	6.69	0.69

Figure 4 presents the two topographic clustering of plots constituting the Quincy vineyard. The first HC considered the altitude, the slope and the U and V exposure, while the second considered the altitude and the slope only. Low altitude plots are concentrated in the north part of the vineyard and near the Cher River, whereas few fields are considered as steep. North-oriented crops concentrate in the middle south of the vineyard, while east oriented are more likely to be found in the northern part.

3.3 Minimum temperatures HC results

Figure 3, Step 3 aims to analyze the temperature distribution according to the type of frost, whether it is advective, radiative, or even a blend of two kinds. As a result, frost risk maps are displayed for each frost type identified, describing the temperature distribution and highlighting hot and cold areas. Some missing data are recorded and marked on cartography.

3.1.1 Comparison of the temperature spatial variability for each type of frost

For each cluster, i.e., for each type of frost night, an HC method has been applied on plots according to the daily minimum temperature recorded. Figure 5 displays the resulting minimum temperature cartographies for each frost situation.

During nights of Cluster 1, extreme plots concentrated in the south of the vineyard, and foremost the extremely cold plots, whereas hot plots were spread widely from north to south.

Temperatures from Cluster 2 were mainly classified as hot or cold temperatures. When speaking about hot and cold temperatures for this situation, it should be noted, however, that the temperatures on nights in Cluster 2 were the highest of the three clusters, thus cannot be compared in terms of magnitude with those of the two other clusters. Most of the average temperatures from clusters 1 and 3 dropped below the average when classified following Cluster 2. Thus, the number of cold plots far exceeds the other two clusters. These were scattered all over the vineyard with an intense concentration northward, on the edge of the Cher River, and in the lower elevations.

During nights from Cluster 3, known as radiative frost nights, some cold plots were noticed in the north part of the vineyard. Three of them were near the Cher River, and one was in a basin that agreed with the theory that cold temperatures flow down the slope to the bottom areas and humidity intake enhances air cooling. Differences could be observed in the spatial variability of temperatures between Cluster 1 and Cluster 3. Four average temperatures from Cluster 1 fall below the average on the third map, two cold temperatures (blue dots on map 1) slightly increased (white dots on map 3), and one southward increased significantly (orange dot on the third map).

The observed slight changes in the temperature spreading highlighted the influence of the synoptic situation (the largest scales) at the local environment scale (micro-scale). Thus, in the Quincy vineyard, radiative situations seemed to cool the northern part of the domain and more specifically plots near a water body, whereas blurred situations, blending advective and radiative frost impacted more severely the southern part of the domain. Nebulosity standardized the temperature and reduced its decline.

It should be highlighted that no matter what kind of frost occurred, some fields were revealed as extremely sensitive or not to the temperature drop.

Figure 6 presents the common hot and cold plots for each type of frost identified. Regardless of the frost situation, eight plots were insensitive to the temperature drop (orange dots), whereas only two were very sensitive (blue dots). Hot fields were spread all over the vineyard, with a high concentration noticed in the south part of the domain. Regarding the cold terrains, one of them was located in a bottom area, and so forth should be affected by katabatic flows, whereas the other was located in a terrain that sinks toward a water body. The lack of dense vegetation near that water body can have enhanced the humidity circulation and increase the frost risk.

3.4 Linking the minimum temperatures and topography HC results: Relationship between temperature distribution topographic situation

Figure 3, Step 4 corresponds to the final step of the HC strategy. This stage is responsible for the final results, i.e., linking the frost type to the temperature distribution across the Quincy vineyard by considering topographic layout.

For each of the topographic HC results (with and without taking U and V exposure into account), the number of common plots between a minimum temperature and a topographic cluster was seeking out. As minimum temperature clusters were already conditioned according to the nature of the frost, it was then possible to observe a relationship between weather variables, the topography and the temperature distribution at micro-scale.

Table 3 shows the comparison between plots clustering following minimum temperatures and topographic parameters altitude, slope, U and V exposure for each type of frost identified previously. Each topographic and temperature cluster is characterized by the prevailing likelihood parameter between plots and compared with one another.

Table 3 Comparison between plots clustering following minimum temperatures and topographic parameters altitude, slope, U and V exposure for each type of frost identified previously

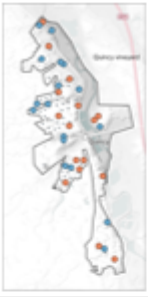
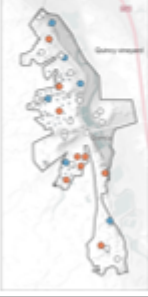
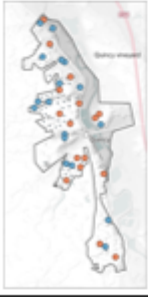
		Cluster 1 Slope ++ Alt --	Cluster 2 U-- V++ (S and E)	Cluster 3 U++ V -- (N and O)	Total	
	Adveective + Radiative situations	Cluster 3 Tmin --	1	2	3	6
		Cluster 1 Tmin avg	13	4	5	22
		Cluster 2 Tmin ++	1	4	4	9
		Total	15/15	10/10	12/12	37
	Radiative + nebulosity situations	Cluster 3 Tmin --	9	3	5	17
		Cluster 2 Tmin ++	4	6	6	16
		Total	13/15	9/10	11/12	33
	Radiative situations	Cluster 3 Tmin --	3	1	2	6
		Cluster 1 Tmin avg	9	4	5	18
		Cluster 2 Tmin ++	1	4	4	9
		Total	13/15	9/10	11/12	33

Table 4 shows the comparison between plots clustering following minimum temperatures and topographic parameters altitude, slope, for each type of frost identified previously. Each topographic and

temperature cluster is characterized by the prevailing likelihood parameter between plots and compared with one another.

Table 4 Comparison between plots clustering following minimum temperatures and topographic parameters altitude and slope for each type of frost identified previously

			Cluster 1 Alt --	Cluster 2 Alt++ Slope--	Cluster 3 Slope ++	Total
	Advection + Radiative situations	Cluster 3 Tmin --	0	5	1	6
		Cluster 1 Tmin avg	8	10	4	22
		Cluster 2 Tmin ++	0	8	1	9
		Total	8/8	23/23	6/6	37
	Radiative + nebulosity situations	Cluster 3 Tmin --	5	8	4	17
		Cluster 2 Tmin ++	2	13	1	16
		Total	7/8	21/23	5/6	33
	Radiative situations	Cluster 3 Tmin --	3	2	1	6
		Cluster 1 Tmin avg	4	11	3	18
		Cluster 2 Tmin ++	0	7	2	9
		Total	7/8	20/23	6/6	33

3.4.1 Blend of advective and radiative situations

It is recalled that the synoptic situation during the nights of Cluster 1 assumed that the frost was plural, with a mixture of advection and radiation. Indeed, the sky was clear and did not evolve; most conditions were anticyclonic or shared between a high and low pressure, and a significant wind from the northeast was noted.

Of the six most severely affected plots (blue dots), three were oriented to the north and northwest, two were oriented to the southeast and south, and one field had a low altitude and high slope. This was

consistent with the fact that the northern plots are more exposed to the advective frost winds, while the western terrains are subject to frost for a more extended period as they do not receive the first rays of the sun. Twenty-two plots constituted a cluster of average temperatures. Low altitudes and high slopes characterized almost 60% of them (13/22). Indeed, low altitude plots are more minor subject to advective frost, while high slopes prevent radiative frost due to katabatic flow.

However, concerning the warm plots, 4/9 were oriented north and northwest and were located on the top of plateaus (low slope and high altitude). These plots could therefore have been subject to advective frost due to their orientation in the first instance and their topographical configuration in the second instance

By studying the location of these plots more precisely, it appeared that two of them were protected by the nearby northern urbanization, whereas another one was surrounded by forest, hence protected from the plateau's strong winds.

The last one, located to the north, should have been sensitive to advective frost. This underlines that although this study shows consistent trends, one additional factor, probably local, escapes us and yet is predominant over all other factors in influencing the temperature distribution. To understand this variability, it seems necessary to refine it at the most local scales to consider the presence of forests, groves, and other slopes that passively redirect temperature flows. In the same way, the humidity provided by a river, a water reserve, or simply the surrounding vegetation should be taken into account, as should the consequences of nearby urbanization (redirection of airflows, drying of the air, or provision of humidity, etc.).

It should be noted that none of the low or high-temperature classes were plots with a low altitude. Also, more than 80% of these two classes were composed of terrains located on plateaus (high altitude, low slope), underlining the plurality of the frost situation.

3.4.2 Cloudy radiative situations

Cluster 2 included both anticyclonic and depressive situations. As a result, the sky was either very heavy or very clear but did not change during the night. Compared to all freezing nights in the dataset, the wind on these nights was medium but from the south and southwest. The situation was either radiative but strongly limited by the cloud cover, or weakly radiative due to the mildness of the weather.

More than 50% of the cold plots had a low or medium altitude and a high slope (9/17). Plots with a steep slope receive more heat during the day and, in addition, may also cool down the most at night. In addition, the katabatic flows had the opportunity to cool down on their way down and affect the plots in their path.

The table 3 shows that exposure was not a predominant parameter in the temperature distribution during this type of frost situation. Indeed, an equal division was noted for the hot plots between the North and/or West and South and/or East orientations. According to the comparison of temperature - topography with

altitude and slope only, more than 80% of the plots (13/16) in the high temperature class had a high altitude and a very low slope (top of the plateau), which is very consistent with the theory. However, it was noticeable that almost 50% (8/17) of the low temperature plots also shared this topographical configuration. If altitude and slope have a similar weight in the cluster characteristics, altitude has nevertheless a significant standard deviation of 4.9m. Thus, the plots in this category can be broken down according to whether they are above or below and close to the overall average (122.4m). Hence, 81% of the warm plots can be divided by 69% (9/13) of the plots with an altitude above the average and 31% (4/13) with an altitude below or close to the average. Similarly for the cold plots, 50% (4/8) of these plots had an altitude above average while the other half have a lower or near average altitude. The same tendency was identified in the comparison with the topographic cluster with low altitudes as it represents 29% of cold plots (5/17) and only 13% of hot plots (2/16). This substantiates the theory that bottom areas are more sensitive to radiative frost. Even if it is not easily identifiable, one can detect the signature of the radiative frost in the temperature spatial variability pattern.

3.4.3 Radiative situations

Nights from Cluster 3 were mainly anticyclonic except one. The sky covered during the night but rarely above 50% (only 2/10 nights) and featured a weak wind from south east. These frost nights were stated as radiative with a light covering of the sky and were also the most typical radiative frost nights that occurred those last three springs. Besides, nights from this cluster were the colder recorded among all the dataset with a mean minimum temperature of -1.82°C .

As was noted for the temperatures in Cluster 2, it would appear that orientation was not a major parameter in the protection of plots against frost, since 44% of the plots with warm temperatures had both a North and/or West and South and/or East exposure. As for the average or low temperatures, there was no strong tendency for the exposure parameters to emerge, contrary to the altitude and slope.

These observations were partially reflected in the second comparison. Indeed, a correspondence was observed between the distribution of cold plots following the two topographical HC results as 50% of plots from cold temperatures cluster were contained in clusters with a low altitude (3/6). Furthermore, none of the plots preserved from the cold had a low altitude. On the contrary, almost 80% of them were located on high plateaus (7/9). However, 61% of the plots with average temperatures were high altitude and low slope plots (11/18), while for the rest, it was more or less 20% in the low altitude (4/18) and high slope clusters (3/18). This result seemed conflicting since following the first topographic HC results, also 50% of this same cluster was found to be part of a low altitude and high slope cluster.

Moreover, for these two classes, the standard deviation by category is significant (see table 2), and it is important to underline the numerous plots constituting the high altitude and low slope cluster (23/37). The 61% and 50% of plots concerned could then be split into a share of plots with below, near and above average altitude. Table 5 presents the comparison of the elevations of the plots from these two topographic clusters constituting the average temperatures cluster. Therefore, for the plots with average temperatures, no clear trend could be seen regarding the altitude.

Table 5 Comparison of the elevations of the plots from the topographic clusters constituting the average temperatures cluster of the radiative frost nights

	Overall share of the cluster Temp avg	Number of plots with below average altitude	Number of plots with close average altitude	Number of plots with above average altitude
Cluster high slope low alt (from HC 1)	9/18	5/9	3/9	1/9
Cluster low slope high alt (from HC 2)	11/18	3/11	3/11	5/11

3.5 Minimum temperature and operation of the wind machines in the Quincy vineyard.

85% of the Quincy vineyard is protected by wind machines. But disparities exist to the point that some plots are equipped with several machines, while others have not been included in the winegrowers' control plan. This configuration makes it possible to compare the temperatures of the protected and unprotected plots, but also to confront the distribution of the machines with the frost-sensitive or non-frost-sensitive zones presented previously.

3.5.1 Comparison between plots equipped or not with wind machines

It appears that out of 37 temperature sensors, 8 of them were farther than 300 m to a wind machine, thus did not catch the effect of a nearby wind machine. In 2021, nights where wind machines operated or not were registered and allowed to monitor the effect of the wind machines park. Hence, it has been possible to compare the mean minimum temperatures

- For plots equipped or not with wind machines
- On frost nights with and without wind machines operation

Table 6 presents the comparison between mean minimum temperature on plots equipped or not with wind machines, during nights when wind machines operated or not. It is apparent that, the plots that are not equipped with a wind machine recorded a colder mean minimum temperature for nights when wind machines were operating comparing to other plots equipped with machines. During nights when wind machines operated, temperatures decreased for both type of plots, equipped or not, with -0.29 °C in average for protected plots and -0.7 °C for unprotected plots. The drop was then more important for plots not equipped with wind machines, but mostly, this temperature was even colder than the one recorded for

plot with wind machines even though the opposite was recording during wind machines free frost nights. For frost nights without WM operation, unprotected plots were hotter by 0.22 °C, whereas for nights with WM operation, the trend reversed with protected plots being hotter than unprotected one by 0.22 °C. Hence, wind machines helped prevailing the temperature to drop too far, while unprotected plots experienced a sharp decrease of temperatures.

Table 6 Comparison between mean minimum temperature on plots equipped or not with wind machines, during nights when wind machines operated or not

	Mean minimum temperature on plots equipped with wind machines	Mean minimum temperature on plots not equipped with wind machines
Frost night without WM operation	-1.18 °C	-0.96 °C
Frost night with WM operation	-1.47 °C	-1.69 °C

3.5.2 Temperature spatial variability and location of wind machines: observations and recommendations.

Wind machines are located throughout the vineyard, with a strong concentration in the center and south-western part, near a branch of the Cher River. The northern and southern parts of the vineyard are moderately equipped, and the eastern part not at all. Comparing the siting of the machines and the study of the temperature spatial variability, it appears that some machines seem well placed, while some areas would need to be either reinforced with additional equipment or equipped with an anti-frost system. Figure 7 represents the location of wind machines and wireless temperature sensors in the vineyard. Hot plots equipped with wind machines are highlighted in brown circles and are therefore zones where one should not invest time and money in frost control. The northern brown circle is a plot equipped with two wind machines while it has been seen previously that this plot is an unsensitive plot to any frost situation. On the contrary, the southern plot within the blue circle should be protected as this plot is particularly sensitive to any frost situation. On the other hand, some unprotected plots, in green on the figure, do not need protection supply, whereas some equipped plots should be better protected (in purple in the figure).

4 Conclusion

The vineyard of Quincy is a site of interest because its topography and its geographical situation offer a suitable terrain to measure spatial variabilities in varied climatic situations, mixing advective, radiative and mixed frosts.

The methodology presented in this paper has made it possible to study the spatial variability of temperatures in the Quincy vineyard from a network of sensors scattered throughout the territory. In addition to this particular field, it is interesting to underline the possible extrapolation of this methodology, since through the installation of a network of temperature sensors, all the parameters used in the present study are available for any other land threatened by spring frost. Moreover, applying the same methodology to several territories allows to increase the number of data and to reinforce the robustness of the HC conclusions.

By combining the 37 temperature sensors and the methodology developed, we were able to identify cold and warm zones for each type of frost. These differ for the most part according to the topography of the terrain. However, if the majority of the distributed temperatures are in agreement with the theory, there are also plots with particular behaviors that remain unexplained in this study. Hence, some plots remain unaffected or on the contrary are very much affected by the drop in temperature. Other plots which would be expected to have a certain temperature result based on their topographic configuration are surprisingly providing the opposite. It is therefore assumed that there are one or more additional factors to be taken into account in order to fully understand the spatial variability of the temperature at the scale of a vineyard. If the wind machines cover today 85% of the vineyard of Quincy, there are nevertheless eight plots which are deprived of it. It has been demonstrated that in 2021, wind machines have reduced the temperature drop compared to the unprotected plots. Furthermore, it appears that the vast majority of the machines are correctly placed. However, consistent with the clustering results, adjustments could be made for more efficient strive. Thus, one plot should be provided with a machine and four others should have their contend means reinforced.

Some limitations appear in this study, especially on the quantity of data which is reduced to the last three seasons, one of which having provided only two nights of frost. Moreover, the coverage of the vineyard in terms of temperature sensors seems modest for the size of the domain. It is therefore difficult to obtain convergent results, but rather to establish a trend. Besides, the weather data were retrieved from a weather station located 22 km from the vineyard, which seems to be significant given the great variability that was observed at local scales. Finally, the study of the effect of the towers could only be analyzed on a few nights of 2021 which, like the previous point, yields a trend rather than converged results.

In perspective of this work, one can note the consideration of further parameters than the minimum temperature. Indeed, the operation of the wind machines is based on the strength of the thermal inversion that is gradually developing after sunset. Therefore, in order to locate the machines in the most efficient places, it seems essential to repeat the same study, taking into account not the minimum temperature in the third step of the clustering, but the strength of the thermal inversion, which is defined as the difference in temperature between 1.5 m and 15 m of height. Our study identifies the plots that need to receive special care in frost protection, and it seems justified to complete it by identifying the areas where the machines are the most efficient, i.e., where the thermal inversion is 1.5°C or more. This would allow to find interesting compromises between the most critical sectors to be protected and the sectors providing the most favorable conditions for the use of wind machines.

Declarations

Fundings

This work was supported by the PEI SICTAG (2019-2020) project funded by the European Commission.

Competing Interests

The authors declare no competing interests.

Authors' Contributions

CLC: Conceptualization; methodology; formal analysis; visualization; writing. DH: Writing; formal analysis. JC: Writing; formal analysis; HQ: Writing; formal analysis; EB: Writing; formal analysis.

Data Availability

The datasets generated and analyzed during the current study are available from the corresponding author on reasonable request.

Code Availability

The code developed for the current study is available from the corresponding author on reasonable request.

Ethics approval

Not applicable.

Consent to participate

Not applicable.

Consent for publication

Not applicable.

References

1. Augspurger, C.K., 2013. Reconstructing patterns of temperature, phenology, and frost damage over 124 years: Spring damage risk is increasing. *Ecology* 94, 41–50. <https://doi.org/10.1890/12-0200.1>
2. Bates, E.M.M., Lombard, P. B., 1978. 5.Evaluation of Temperature Inversions and Wind Machine on Frost Protection in Southern Oregon. *Agric. Exp. Sta. Spec. Rep.* 514 19.
3. Battany, M.C., 2012. Vineyard frost protection with upward-blowing wind machines. *Agric. For. Meteorol.* 157, 39–48. <https://doi.org/10.1016/j.agrformet.2012.01.009>

4. Beyá-Marshall, V., Herrera, J., Santibáñez, F., Fichet, T., 2019. Microclimate modification under the effect of stationary and portable wind machines. *Agric. For. Meteorol.* 269–270, 351–363.
<https://doi.org/10.1016/j.agrformet.2019.01.042>
5. Brooks, F.A., Kepner, R.A., Yerg, D.G., n.d. Wind {Machines} in {Orchards} 2.
6. Cittadini, E.D., de Ridder, N., Peri, P.L., van Keulen, H., 2006. A method for assessing frost damage risk in sweet cherry orchards of South Patagonia. *Agric. For. Meteorol.* 141, 235–243.
<https://doi.org/10.1016/j.agrformet.2006.10.011>
7. Detzer, J., Loikith, P.C., Pampuch, L.A., Mechoso, C.R., Barkhordarian, A., Lee, H., 2020. Characterizing monthly temperature variability states and associated meteorology across southern South America. *Int. J. Climatol.* 40, 492–508. <https://doi.org/10.1002/joc.6224>
8. Doesken, N.J., McKee, T.B., 1988. A climatological assessment of the utility of wind machine for freeze protection in mountain valleys. *J. Appl. Meteorol.* 28.
9. Evans, R.G., 2000. The Art of Protecting Grapevines From Low Temperature Injury. *Proc. ASEV 50th Anniv. Meet.* June 19-23 60–72.
10. Gavrilescu, C., Bois, B., Larmure, A., Ouvre, M., Richard, Y., 2019. Analyse Spatiale De L'Évolution Du Risque De Gel Sur La Vigne En Bourgogne-Franche-Comté. XXXIIème Colloq. Int. l'AIC 181–185.
11. Gobbett, D.L., Nidumolu, U., Crimp, S., 2020. Modelling frost generates insights for managing risk of minimum temperature extremes. *Weather Clim. Extrem.* 27, 100176.
<https://doi.org/10.1016/j.wace.2018.06.003>
12. Heusinkveld, V.W.J., van Hooft, J., Schilperoort, B., Baas, P., Veldhuis, M. ten, van de Wiel, B.J.H., 2020. Towards a physics-based understanding of fruit frost protection using wind machines. *Agric. For. Meteorol.* 282–283, 107868. <https://doi.org/10.1016/j.agrformet.2019.107868>
13. Jackson, R.S., 2000. Grapevine Structure and Function. *Wine Sci.* 45–95.
<https://doi.org/10.1016/b978-012379062-0/50004-4>
14. Jones, G. V., Davis, R.E., 2000. Climate influences on grapevine phenology, grape composition, and wine production and quality for Bordeaux, France. *Am. J. Enol. Vitic.* 51, 249–261.
15. Kalma, J.D., Laughlin, G.P., Caprio, J.M., Hamer, P.J.C., 1992. The {Bioclimatology} of {Frost}: {Its} {Occurrence}, {Impact} and {Protection}, *Advances in {Bioclimatology}*. Springer Berlin Heidelberg, Berlin, Heidelberg. <https://doi.org/10.1007/978-3-642-58132-8>
16. Lakatos, L., Hadvári, M., Szél, J., Gonda, I., Szabó, Z., Soltész, M., Sun, Z., Zhang, J., Nyéki, J., Szukics, J., 2016. Technologies developed to avoid frost damages caused by late frost during bloom in the fruit growing regions of Siófok and Debrecen. *Int. J. Hortic. Sci.* 18, 99–105.
<https://doi.org/10.31421/ijhs/18/2/1040>
17. Le Roux, R., 2017. Modélisation climatique à l' échelle des terroirs viticoles dans un contexte de changement climatique 207.
18. Leolini, L., Moriondo, M., Fila, G., Costafreda-Aumedes, S., Ferrise, R., Bindi, M., 2018. Late spring frost impacts on future grapevine distribution in Europe. *F. Crop. Res.* 222, 197–208.
<https://doi.org/10.1016/j.fcr.2017.11.018>

19. Ma, Q., Huang, J.G., Hänninen, H., Berninger, F., 2019. Divergent trends in the risk of spring frost damage to trees in Europe with recent warming. *Glob. Chang. Biol.* 25, 351–360.
<https://doi.org/10.1111/gcb.14479>
20. Meier, M., Fuhrer, J., Holzkämper, A., 2018. Changing risk of spring frost damage in grapevines due to climate change? A case study in the Swiss Rhone Valley. *Int. J. Biometeorol.* 62, 991–1002.
<https://doi.org/10.1007/s00484-018-1501-y>
21. Mosedale, J.R., Wilson, R.J., Maclean, I.M.D., 2015. Climate change and crop exposure to adverse weather: Changes to frost risk and grapevine flowering conditions. *PLoS One* 10, 1–16.
<https://doi.org/10.1371/journal.pone.0141218>
22. Murtagh, F., Contreras, P., 2012. Algorithms for hierarchical clustering: An overview. *Wiley Interdiscip. Rev. Data Min. Knowl. Discov.* 2, 86–97. <https://doi.org/10.1002/widm.53>
23. Quénel, H., Monteiro, A., Beltrando, G., Maciel, A., 2004. Mesures climatiques aux échelles fines (météorologiques et agronomiques) et variabilité spatiale du gel printanier dans le vignoble de Vinho Verde (Portugal). *Norois* 117–132. <https://doi.org/10.4000/norois.826>
24. Ribeiro, A.C., De Melo-Abreu, J.P., Snyder, R.L., 2006. Apple orchard frost protection with wind machine operation. *Agric. For. Meteorol.* 141, 71–81.
<https://doi.org/10.1016/j.agrformet.2006.08.019>
25. Sgubin, G., Swingedouw, D., Dayon, G., García de Cortázar-Atauri, I., Ollat, N., Pagé, C., van Leeuwen, C., 2018. The risk of tardive frost damage in French vineyards in a changing climate. *Agric. For. Meteorol.* 250–251, 226–242. <https://doi.org/10.1016/j.agrformet.2017.12.253>
26. Small, R.T., 1949. of the.
27. Snyder, R.L., de Melo-Abreu, J.P., 2005. fundamentals, practice and economics 1, 240.
28. Snyder, R.L., Melo-Abreu, J.P. de, 2005. Frost protection: fundamentals, practice and economics, Environment and natural resources series. Food and Agriculture Organization of the United Nations, Rome.
29. Unterberger, C., Brunner, L., Nabernegg, S., Steininger, K.W., Steiner, A.K., Stabentheiner, E., Monschein, S., Truhetz, H., 2018. Spring frost risk for regional apple production under a warmer climate. *PLoS One* 13, 1–18. <https://doi.org/10.1371/journal.pone.0200201>
30. Van Oldenborgh, G.J., Li, S., 2022. Human influence on growing period frosts like the early april 2021 in Central France 1–25.
31. Webb, M., Pirie, A., Kidd, D., Minasny, B., 2018. Spatial analysis of frost risk to determine viticulture suitability in Tasmania, Australia. *Aust. J. Grape Wine Res.* 24, 219–233.
<https://doi.org/10.1111/ajgw.12314>
32. Zohner, C.M., Mo, L., Renner, S.S., Svenning, J.C., Vitasse, Y., Benito, B.M., Ordonez, A., Baumgarten, F., Bastin, J.F., Sebald, V., Reich, P.B., Liang, J., Nabuurs, G.J., De-Miguel, S., Alberti, G., Antón-Fernández, C., Balazy, R., Brändli, U.B., Chen, H.Y.H., Chisholm, C., Cienciala, E., Dayanandan, S., Fayle, T.M., Frizzera, L., Gianelle, D., Jagodzinski, A.M., Jaroszewicz, B., Jucker, T., Kepfer-Rojas, S., Khan, M.L., Kim, H.S., Korjus, H., Johannsen, V.K., Laarmann, D., Langn, M., Zawila-Niedzwiecki, T., Niklaus, P.A.,

Paquette, A., Pretzsch, H., Saikia, P., Schall, P., Seben, V., Svoboda, M., Tikhonova, E., Viana, H., Zhang, C., Zhao, X., Crowther, T.W., 2020. Late-spring frost risk between 1959 and 2017 decreased in North America but increased in Europe and Asia. Proc. Natl. Acad. Sci. U. S. A. 117. <https://doi.org/10.1073/pnas.1920816117>

Figures

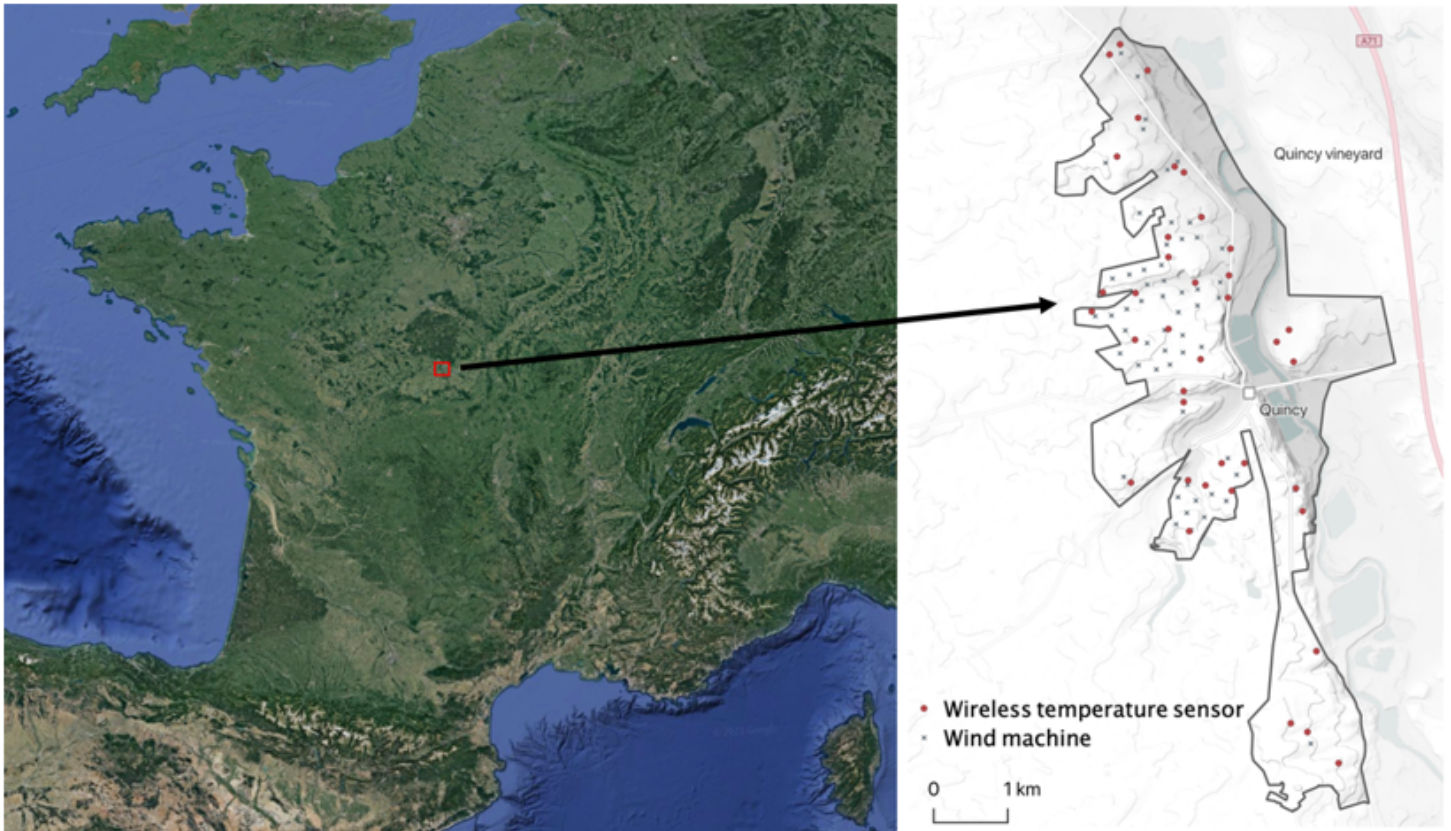


Figure 1

Left: Location of the vineyard of Quincy in France. Right: Map of the Quincy vineyard with locations of wind machines (red dots) and temperature sensors (blue dots). Borders are delimited with solid black lines

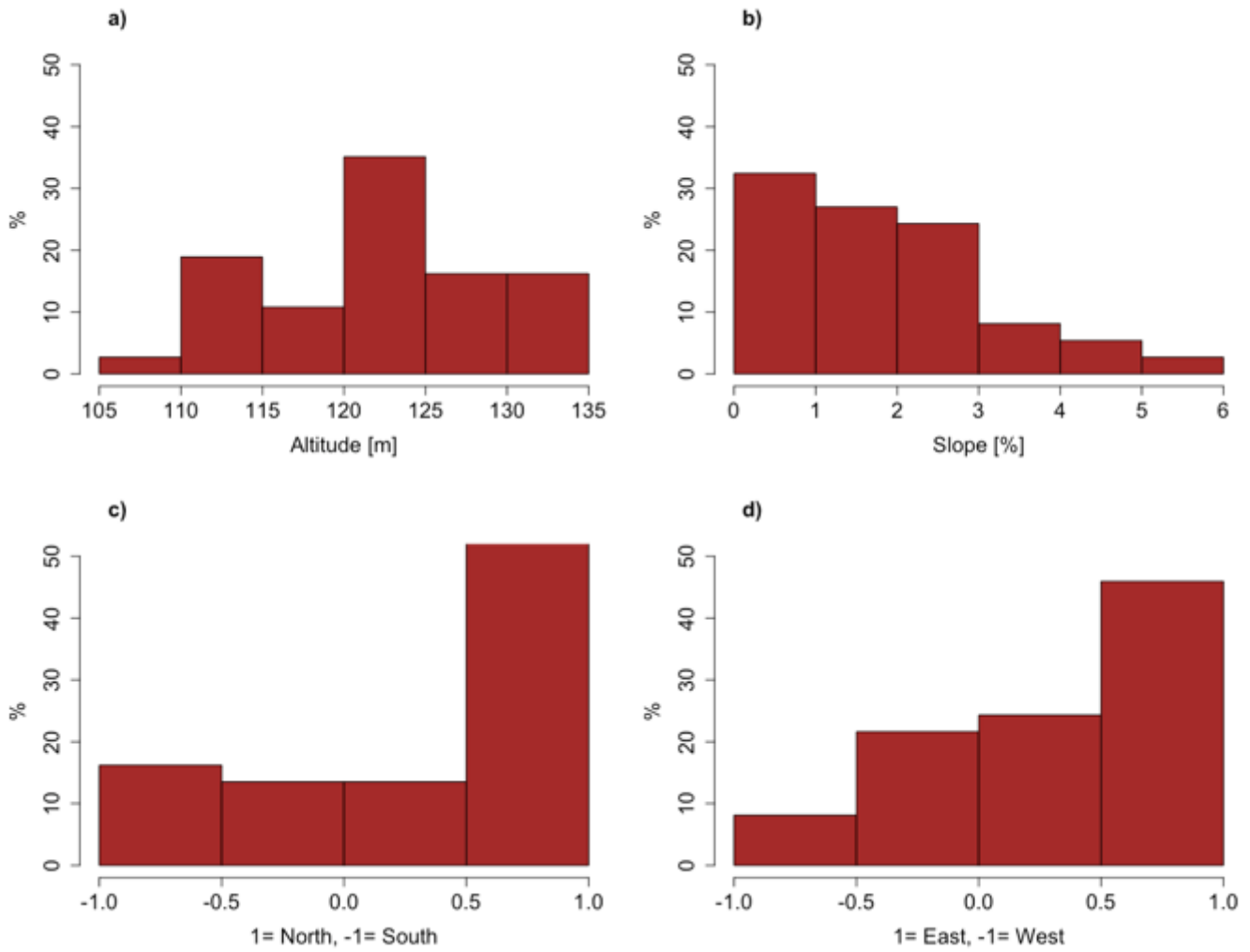


Figure 2

Histograms of the topographic data at sensor locations in the Quincy vineyard showing the frequency of plots following the: a) elevation, b) slope, c) U orientation, d) V orientation. The data source is a 5-m accurate DEM from French National Institute of Geographic Information

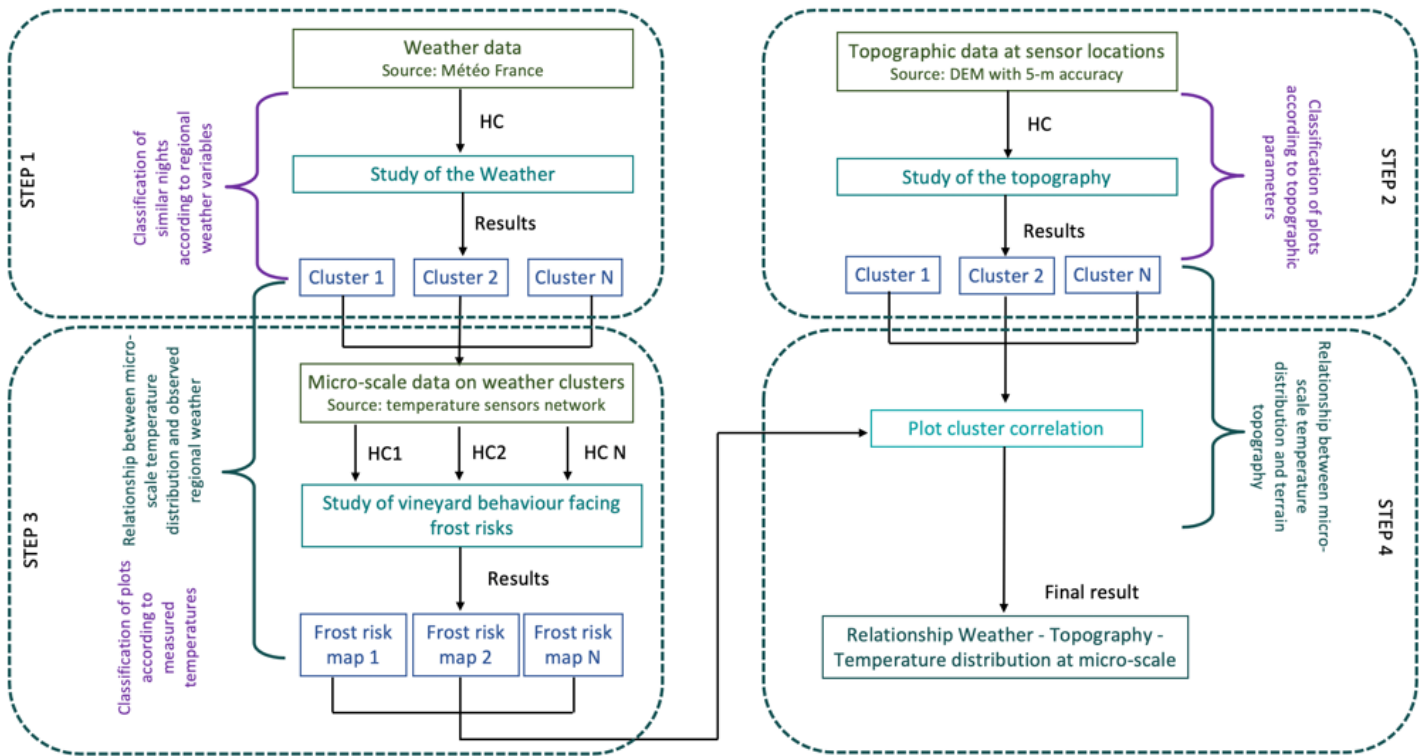


Figure 3

Scheme of hierarchical clustering analyze strategy to study the temperature spatial variability in the Quincy vineyard during frost events

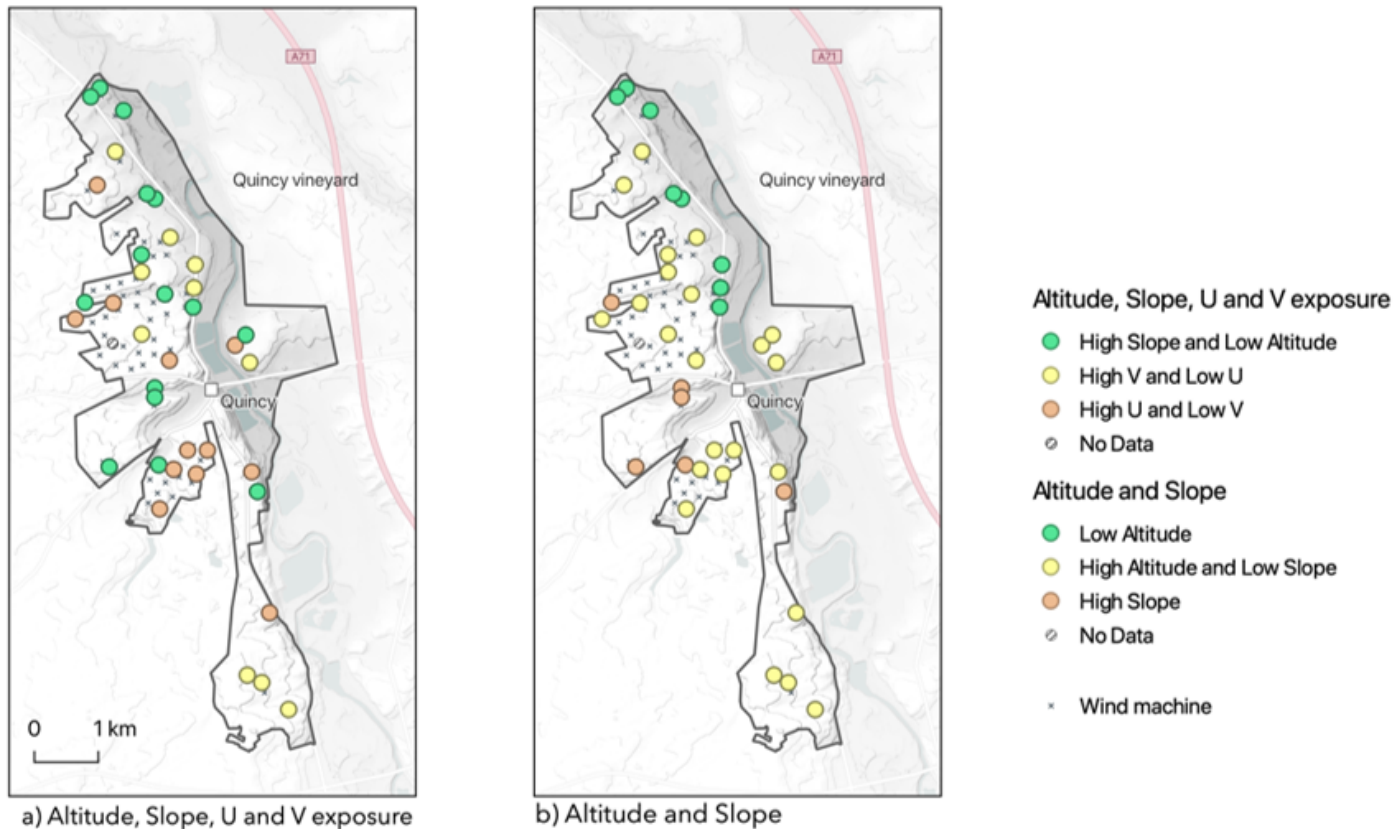


Figure 4

Topographic clustering of plots in the Quincy vineyard. Defined at temperature sensor locations from 5-m accurate DEM.

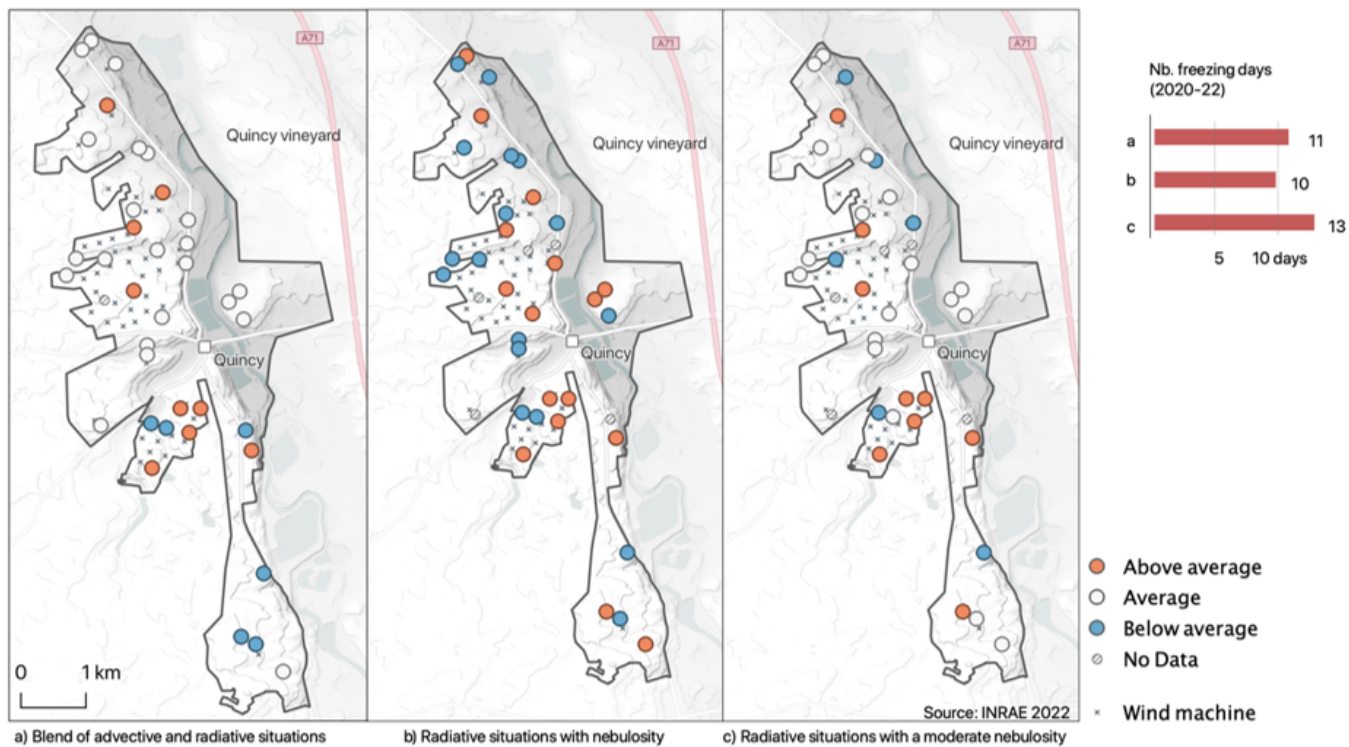


Figure 5

Cartographies of the temperature spatial variability for different types of frost in the Quincy vineyard for a) mixed frost situations, b) radiative situations with significant nebulosity and c) radiative situations with a light nebulosity

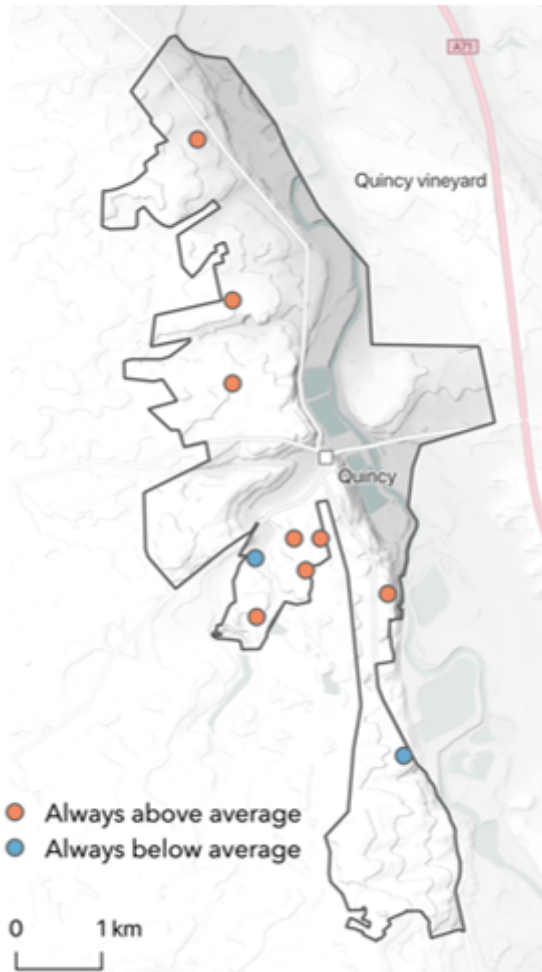


Figure 6

Common hot and cold plots for each type of frost identified

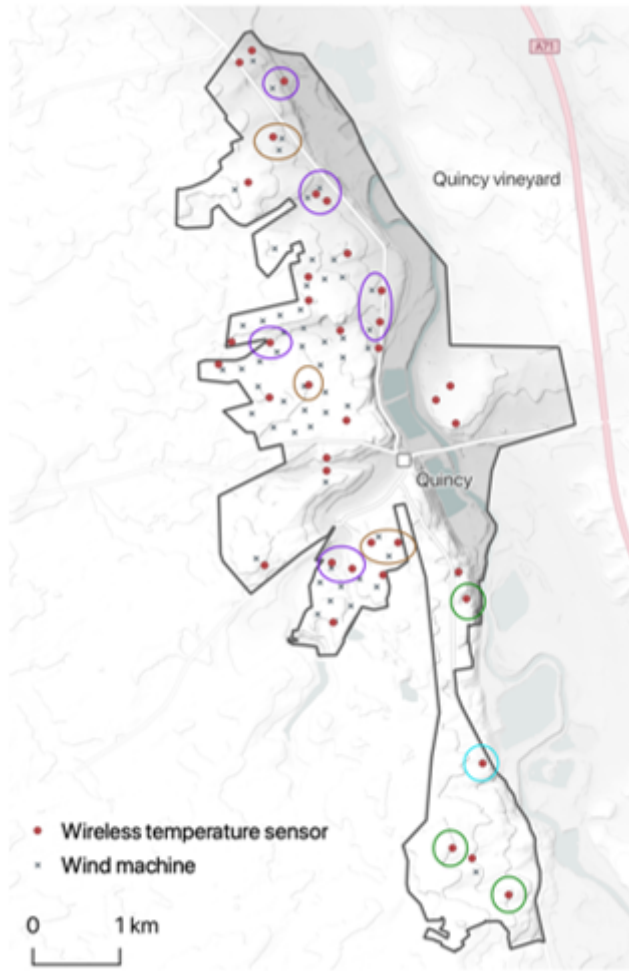


Figure 7

Recommendation on wind machines locations throughout the Quincy vineyard. Green circles represent plots without WM and which do not need it. Plot within the blue circle should be provided with a frost control system as well as plots within purple circles should receive extra frost control supplies. Finally, plots within brown circles should receive less attention in the frost fight